Progress In Electromagnetics Research C, Vol. 124, 211–225, 2022

A Fast Prediction Method for the Radio Propagation under the Obstacle Environment

Ceyi Ma[1], Yinghong Wen[1, 2], Jinbao Zhang[1, 2, *], and Dan Zhang[1]

Abstract—To rapidly simulate the forward electromagnetic scattering of multiple obstacles, we propose a new forward scattering prediction model, which can effectively simulate the propagation of electromagnetic waves in a large-scale environment, accurately calculate the scattering of multi-scale structures, and realize multi-region parallel computation. Specifically, the proposed model consists of an obstacle region and a large-scale environment region. To make the model consistent with the real scene quickly and accurately, the time-domain parabolic equation (TDPE) and discontinuous Galerkin time-domain (DGTD) method are employed to simulate the propagation of electromagnetic waves and the scattering of obstacles, respectively. At the same time, each region is equivalent to a linear time-invariant (LTI) system, and the transfer function of each system is calculated by the discrete Laplace Z-transform to realize multi-region parallel computation. This model can simulate the propagation of the electromagnetic wave in multiple obstacles more quickly under large-scale background than the existing obstacle forward scattering model. Numerical results demonstrate that the proposed model is effective in terms of accuracy and runtime performance.

1. INTRODUCTION

Electromagnetic wave propagation simulation in a large-scale background environment is of great significance for satellite navigation simulation [1], radar echo [2], radio communication [3], and other fields. At present, there are three problems in electromagnetic wave propagation simulation technology in a novel large-scale environment with multi-scale obstacles. Firstly, the calculation efficiency and accuracy of multi-scale obstacle scattering in a large-scale environment are taken into account. Secondly, The complex connection between processing regions makes it difficult to implement the hybrid algorithm. Thirdly, the process of parallel computing is simplified.

In this paper, the main goal is to design a hybrid algorithm, including the discontinuous Galerkin time-domain (DGTD), time-domain parabolic equation (TDPE) methods, and Z-transform, which is capable of predicting electromagnetic wave propagation over irregular terrain or flat terrain with various obstacles.

Considering the numerical accuracy and computational efficiency of electromagnetic wave propagation simulation, the parabolic equation (PE) method is usually used to calculate the electromagnetic wave propagation in a large-scale environment, and the FDTD method is used to calculate the scattering of obstacles. The hybrid FDTD-PE method is raised in [4] to predict the distribution of additional secondary factors (ASFs) in situations with near-source complex topography. Nevertheless, it is worth noting that the hybrid FDTD-PE model is a 2D model. Due to the neglect of the lateral effects, using 2D model for Loran-C ASF prediction in realistic 3D environments would inevitably introduce errors, especially for 3D topography with severe lateral changes. In addition, although the boundary integral equation method mentioned in [5] about the scattering of high-frequency plane waves

Received 17 August 2022, Accepted 16 September 2022, Scheduled 28 September 2022

* Corresponding author: Jinbao Zhang (jbzhang@bjtu.edu.cn).

[1] Beijing Jiaotong University, Beijing 100044, China. [2] Frontiers Science Center for Smart High-speed Railway System (SHRS), Beijing 100044, China.

by perfect conductive obstacles can accurately calculate the scattering problem of obstacles, it still needs the accelerated calculation of iterative methods such as GMRES to ensure the efficiency. In fact, the traditional boundary integral (BI) method and the Method of Moments (MoM), which are still inefficient in multi-scale structures calculation, are not suitable for wide-band scattering problems.

With regard to the transition problem, FDTD/PE hybrid method in [6] is discussed, which carefully selects the distance location of the transition field value extracted from the FDTD region according to the obstacle's structure. However, the use of this method needs to satisfy two preconditions: firstly, the field near the PML layer of the transition plane should be as smooth as possible; secondly, the field accumulated on the transition plane should be within the effective region of the paraxial method. Therefore, this method is very limited and complicated in practical application. In addition to the boundary treatment scheme of FDTD/PE hybrid method, similar schemes can be found in other mixed numerical methods. In [7], a buffer is used to implement the coupling between FDTD and FETD regions. In [8], there is a cubic layer between the SETD region and the FDTD region, and an explicit SETD/FDTD hybrid approach is put forward. Furthermore, an implicit and explicit time integration scheme is proposed to eliminate buffers that can cause an increase in time and memory consumption [9]. In addition to buffers, there are several approaches to the boundary continuity problem in the domain decomposition method (DDM), such as introducing an auxiliary current into the interface of different subdomains of FEM and the interface of FEM subdomains with BEM subdomains [10]. Meanwhile, it can be applied to the scattering of composites. In [11], the Robin transmission condition (RTC) is used to deal with the field continuity between multi-layered media, which takes into account the mutual coupling between adjacent subdomains, making the DDM system a highly sparse matrix. In paper [12], the solution region is decomposed into multiple sub-regions, and FFT is used to accelerate the self-coupling and mutual coupling among sub-regions. However, for those cases with a large-scale difference in the x or y-direction, this method does not have obvious advantages. Additionally, the large cell numbers along the z-direction would result in significantly high memory cost and low computation speed.

For parallel computing, in paper [13], multiple GPUs are used to accelerate alternating-direction-implicit FDTD (ADI-FDTD) method based on domain decomposition technique, which, however, requires high-performance computers and brings high hardware cost. The implicit updating equations of the FDTD method in [14] could be solved simultaneously by multithreading, which can effectively speed up the solution process. As a method to improve computing efficiency, parallel computing has been widely used in the field of numerical computing. In [15], a parallel FDTD/ADI-PE method for ultra-large-scale electromagnetic simulation on a distributed computing platform is proposed, which further reduces the transfer data size by using the sparsity of the tridiagonal matrices. However, the parallel FDTD/ADI-PE method needs to deal with the data transmission between multiple cores, and the implementation process is complicated. Meanwhile, although the above parallel computing method can improve the solving rate, it is very complicated in the implementation process for the need to deal with data transmission between multiple cores and has high requirements on the computer performance for the need to deal with data transmission problems in multiple regions at the same time. Particularly, for non-computer professionals, the implementation process is more complicated.

In this paper, the TDPE method is used to calculate the propagation of electromagnetic waves in a large-scale environment. Since the DGTD method is more suitable for multi-scale structure obstacles than the FDTD method [16], the forward scattering of obstacles is calculated by the DGTD method. To simplify the connection between obstacles and reduce the complexity of the parallel computing process, this paper considers using Z-transform to characterize the forward scattering characteristics of each obstacle. The Z-transform has been applied to FDTD methods before [17–20]. The Z-FDTD method is mainly used to calculate the scattering and wave propagation of dispersive media [21–25]. However, there are few studies on using Z-transform to predict electromagnetic wave propagation with multiple obstacles.

The rest of this article is structured as follows. In Section 2, a hybrid method is introduced. In Section 3, the proposed method is used to calculate the forward scattering of obstacles with different structures, and the effectiveness of this method is verified. In Section 4, the prediction accuracy and applicable conditions of different excitation sources, double obstacle model, and multi-scale model are discussed. In Section 5, a summary is provided.

2. FORMULAS OF HYBRID METHODS

This section mainly discusses a kind of simple and feasible method of parallel computing. The region can be divided into large-scale background and obstacles, and then different methods are used for their respective regions to calculate the output signal and calculate the system transfer function of each region at the same time. Finally, the forward scattering of the whole region is calculated according to the initial excitation signal by multiplying each transfer function.

2.1. TDPE-DGTD Hybrid Prediction Model

We regard the electromagnetic wave propagation with obstacles as a linear time-invariant system. Meanwhile, as shown in Fig. 1, we decompose the whole system into several subsystems and use the TDPE method and DGTD method to calculate the subsystem transfer function of each region.

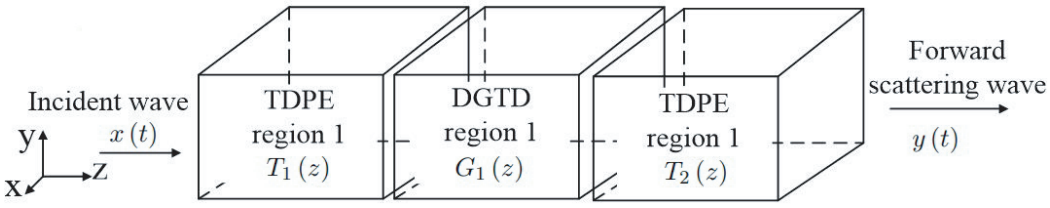

Figure 1. Schematic diagram of multi-obstacles forward scattering prediction model.

Specific to each system, the excitation source is consistent. Since each sub-region is a linear time-invariant system, the transfer function can be solved in each sub-region at the same time, to realize parallel computing.

$$y(t) = \mathrm{Z}^{-1}\left\{ x(z) \prod_{\mathrm{i}=1}^{\mathrm{n}} T_{\mathrm{i}}(z) \prod_{\mathrm{j}=1}^{\mathrm{m}} G_{\mathrm{j}}(z) \right\} \tag{1}$$

where $x(z)$ is the Z-transform of the incident wave excitation $x(t)$.

T_{i} and G_{j} correspond to the transfer functions of each subsystem respectively.

$$T_{\mathrm{i}}(z) = \frac{y_{\mathrm{i}}(z)}{x(z)} \tag{2}$$

$$G_{\mathrm{j}}(z) = \frac{y_{\mathrm{j}}(z)}{x(z)} \tag{3}$$

where $y_{\mathrm{i}}(z)$ and $y_{\mathrm{j}}(z)$ respectively correspond to the output signal of the radio wave propagation region and obstacle region.

The above prediction model assumes that the obstacles are far enough apart to ignore the mutual coupling between the obstacles.

2.2. 3D-TDPE method

The 3D wave equation can be expressed as:

$$\frac{\partial^2 \Psi}{\partial x^2} + \frac{\partial^2 \Psi}{\partial y^2} + \frac{\partial^2 \Psi}{\partial z^2} + k_0^2 n^2 \Psi = 0 \tag{4}$$

where Ψ is the components scattered field, meanwhile, and k_0 and n correspond to the wave number in free space and the refractive index.

The 3D forward propagation PE is obtained by factorization using the Feit-Fleck approximation:

$$\frac{\partial \Psi}{\partial z} + i\left[\sqrt{k_0^2 - k_x^2 - k_y^2} + k_0(n-1)\right] = 0 \tag{5}$$

The split-step Fourier transform (SSFT) method is used to solve PE:

$$\Psi(x,y,z+\Delta z,f)=\Im_s^{-1}\left\{e^{j\sqrt{k_0^2-k_x^2-k_y^2}\Delta z}\Im_s\left[e^{jk_0(n-1)\Delta z}\Psi(x,y,z,f)\right]\right\} \tag{6}$$

where $\Im_s$ and $\Im_s^{-1}$ represent the Fourier transform (FT) and inverse Fourier transform (IFT), respectively. Then, the time domain parabolic equation (TDPE) can be obtained by:

$$\Psi(x,y,z,t)=\sum_{k=0}^{N-1}A(f)\,\Psi(x,y,z,f)\,e^{-j2\pi ft} \tag{7}$$

2.3. DGTD Method

For the scattering solution in the obstacle area, the electromagnetic wave propagating to the area near the obstacle obtained by the TDPE method was used as the excitation source to solve the Huygens surface surrounding the obstacle area as shown in Fig. 2 and to solve the induced current and induced magnetic current on the surface. Then, the DGTD method is used to solve the electromagnetic wave scattering field caused by obstacles.

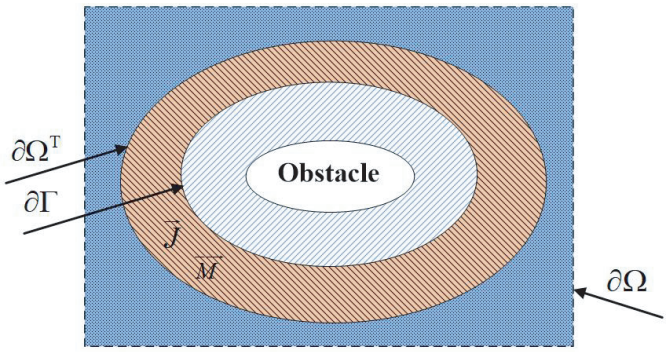

Figure 2. Schematic diagram of the obstacle region boundary $\partial\Omega$, TF/SF surface $\partial\Omega^{\mathrm{T}}$, and Huygens' surface $\partial\Gamma$.

After calculating the scattering field, we can obtain the system transfer function $G(z)$ of the obstacle. The DGTD algorithm used is based on [26].

3. VALIDATION OF HYBRID METHOD

In Section 3, to analyze the applicability and effectiveness of the proposed method, the linear time-invariance of the system, the influence of excitation source characteristics on the prediction accuracy and the forward scattering prediction for multiple obstacles are discussed. In addition, the environment involved in all subsequent simulations is set as free space.

3.1. Verification of LTI Property of Forward Scattering Prediction Model

We use TDPE-DGTD hybrid method to calculate the propagation of electromagnetic wave and forward scattering of different obstacles, respectively, and then the TDPE and DGTD are used to calculate the output signals of each subdomain. The input and output signals of each subdomain are used to calculate the system transfer function of each subdomain through the system identification module in MATLAB.

We define the excitation source as a sinusoidal modulated Gaussian pulse signal:

$$x(t)=Ae^{-\left(\frac{t-t_0}{T}\right)}\sin 2\pi f_0(t-t_0) \tag{8}$$

Firstly, we discuss the LTI of the obstacle forward scattering system. We consider the incident wave $A=1\,\mathrm{V/m}$, $T=2.6\,\mathrm{ns}$, $t_0=15\,\mathrm{ns}$, and $f_c=500\,\mathrm{MHz}$.

Then, the DGTD method is used to calculate the forward scattering of the three models. The excitation signal is used as the system input, and the forward scattering is used as the system output to import into the MATLAB system identification module, which can quickly obtain the system transfer function (STF):

$$\begin{cases} STF_{\text{cube}} \dfrac{\begin{array}{l}126.2z^{-1}-598.6z^{-2}+734z^{-3}+177.1z^{-4}\\ -591.9z^{-5}-293.7z^{-6}+465.2z^{-7}+377.3z^{-8}\\ -567.5z^{-9}+171.8z^{-10}\end{array}}{1+0.1292z^{-1}-0.8708z^{-2}} \\ STF_{\text{sphere}} = \dfrac{\begin{array}{l}-1212z^{-1}-5948z^{-2}-8630z^{-3}-3108z^{-4}\\ +2.035\times10^{4}z^{-5}-1.62\times10^{4}z^{-6}-5622z^{-7}\\ +1.553\times10^{4}z^{-8}-8758z^{-9}+1702z^{-10}\end{array}}{1-0.8282z^{-1}-0.1306z^{-2}} \\ STF_{\text{cone}} = \dfrac{\begin{array}{l}38.18z^{-1}-144.6z^{-2}+179.9z^{-3}-52.53z^{-4}-32.4z^{-5}\\ -4.473z^{-6}-11.57z^{-7}+69.87z^{-8}-56.1z^{-9}+13.73z^{-10}\end{array}}{1-2.935z^{-1}+2.877z^{-2}-0.9415z^{-3}} \end{cases} \tag{9}$$

Then, the incident wave parameters $A = 3\,\text{V/m}$, $T = 2.6\,\text{ns}$, $t_0 = 15\,\text{ns}$, and $f_c = 500\,\text{MHz}$ are changed, and the new incident wave is used as the input to calculate the predicted value by using the system transfer function. Meanwhile, the results calculated by the CST simulation software were used as a reference. The dimensions of the cube are $1\,\text{m} \times 1\,\text{m} \times 1\,\text{m}$. The base of the cone has a radius of 0.5 m and a height of 1.5 m. The radius of the sphere is 1 m.

Additionally, we superimpose two sinusoidal modulated Gaussian pulse signals with different amplitude and delay to discuss the time-invariance of LTI system.

As shown in Fig. 3 and Fig. 4, after the amplitude and phase of the incident wave are changed, the prediction results are in good agreement with the reference ones obtained by CST simulation software.

Meanwhile, according to the error analysis in Table 1, for the forward scattering of different structural obstacles, the MSE (Mean Square Error) of the proposed method is all below 10^{-6}.

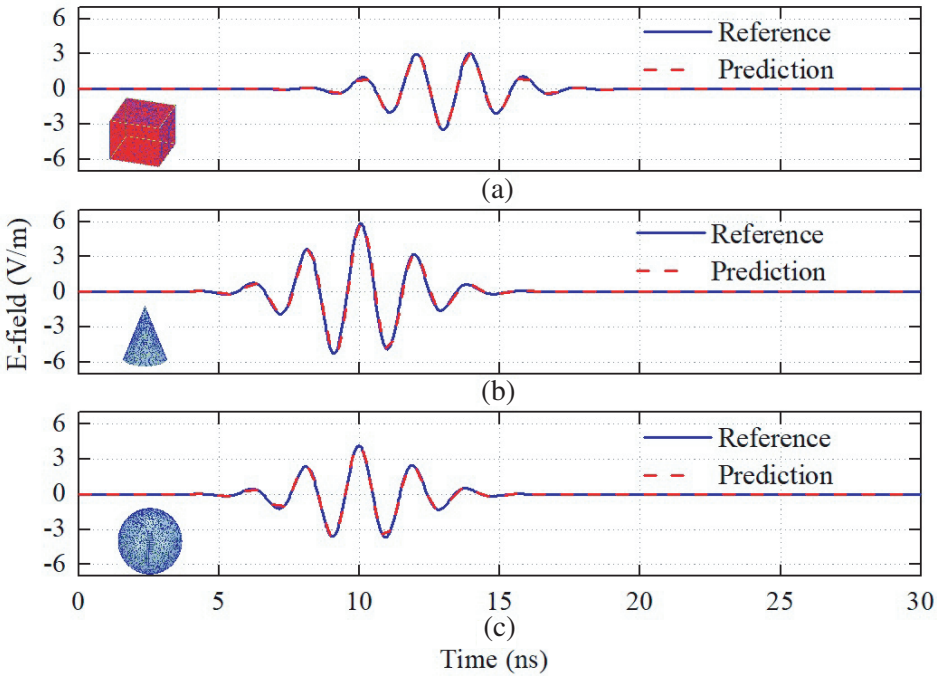

Figure 3. Prediction of forward scattering of (a) cube, (b) cone and (c) sphere obstacles in 500 MHz.

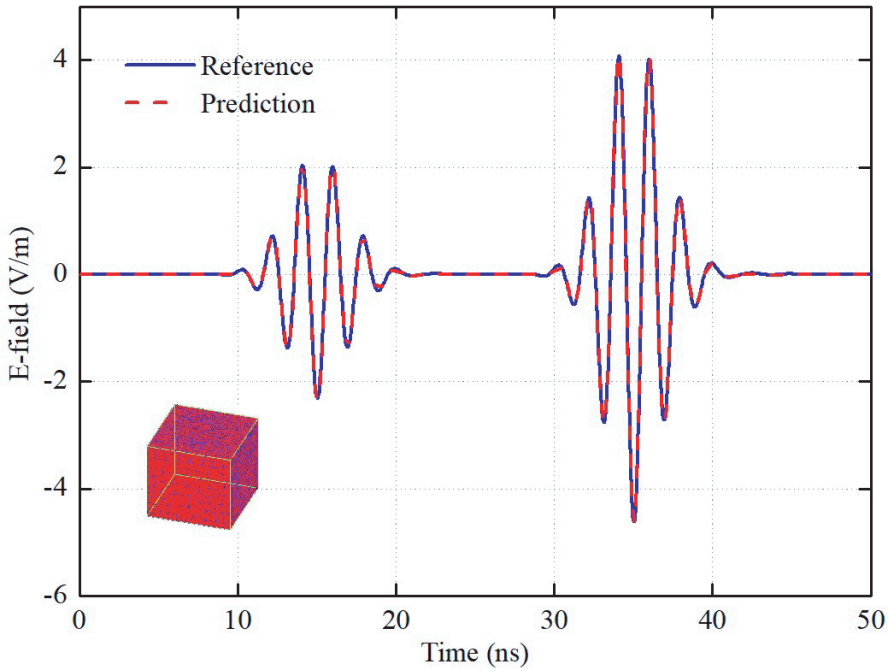

Figure 4. Influence of superposition of excitation sources on the predictability of forward scattering systems.

Table 1. MSE of forward scattering prediction of cube, cone and sphere obstacles in 500 MHz.

Type of obstacle	Mean Square Error (MSE)
Cube	5.8182e-7
Cone	2.0224e-8
Sphere	9.5380e-6

3.2. Verification of the Forward Scattering Prediction Model for Different Spectral

In fact, sometimes we need to discuss radio wave propagation from excitation sources with different signal bandwidths. In general, the traditional algorithms resolve this process, which leads to repeated simulation and increase of the time cost. Since the transfer function depends on the characteristics of the system and is independent of the input signal waveform, the TDPE-DGTD hybrid method proposed in this paper can predict the wave propagation characteristics of other signals with different bandwidths based on the known transfer function, so as to effectively reduce the repetitive work caused by multiple simulations. At the same time, this scheme not only is limited to the hybrid algorithm mentioned in this paper, but also can be applied to other hybrid algorithms.

Therefore, in addition to the analysis of linear time-invariant characteristics in Section 3.1, we also discuss the influence of the variation of excitation source center frequency and frequency bandwidth on the prediction of the proposed method.

Specifically, we first use a sinusoidal modulated gaussian pulse with a center frequency of 500 MHz and $T = 2.6$ ns as the excitation source to solve the transfer function of the area where the obstacle is located, and then predict the forward scattering with a center frequency of 750 MHz and $T = 5$ ns based on this transfer function.

As shown in Fig. 5 and Table 2, when the spectrum is changed, the prediction results are still consistent with the reference values, and MSE can be kept in the range of 10^{-7} to 10^{-3}.

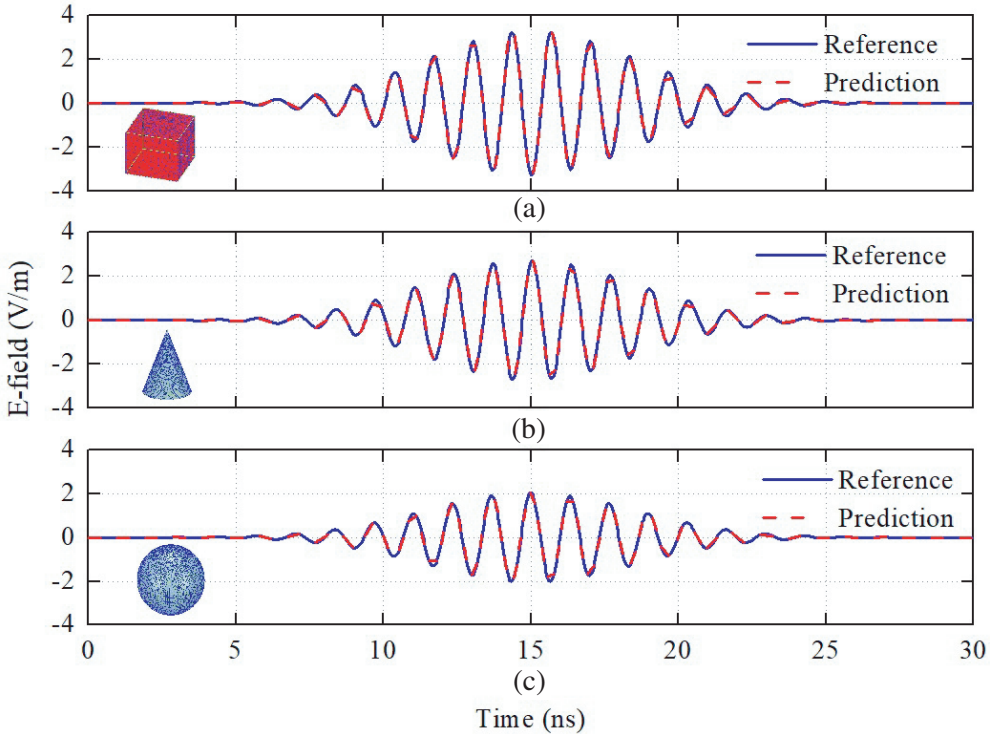

Figure 5. Prediction of forward scattering of (a) cube, (b) cone and (c) sphere obstacles in 750 MHz.

Table 2. MSE of forward scattering prediction of cube, cone and sphere obstacles in 750 MHz.

Type of obstacle	Mean Square Error (MSE)
Cube	2.36e-03
Cone	4.29e-05
Sphere	3.24e-07

3.3. Verification of the Forward Scattering Prediction Model for Different Excitation Sources

In addition to the previous sinusoidal modulated Gaussian pulse, this part also discusses the sine wave and Gaussian pulse excitation source and analyzes their MSE. The transfer function adopts Eq. (9).

As shown in Fig. 6, the frequency of the sine wave is 500 MHz; the pulse width of the Gaussian pulse signal is 1.8 ns; the pulse delay is 5 ns.

As shown in Fig. 7 and Table 3, for three different excitation sources, the forward scattering prediction model can achieve very low MSE. The above results show that the prediction model is suitable for different excitation sources.

Table 3. MSE of forward scattering prediction model for different excitation sources.

Type of excitation source	Mean Square Error (MSE)
Sinusoidal modulated Gaussian pulse	9.54e-6
Sine wave	6.23e-7
Gaussian pulse	6.45e-6

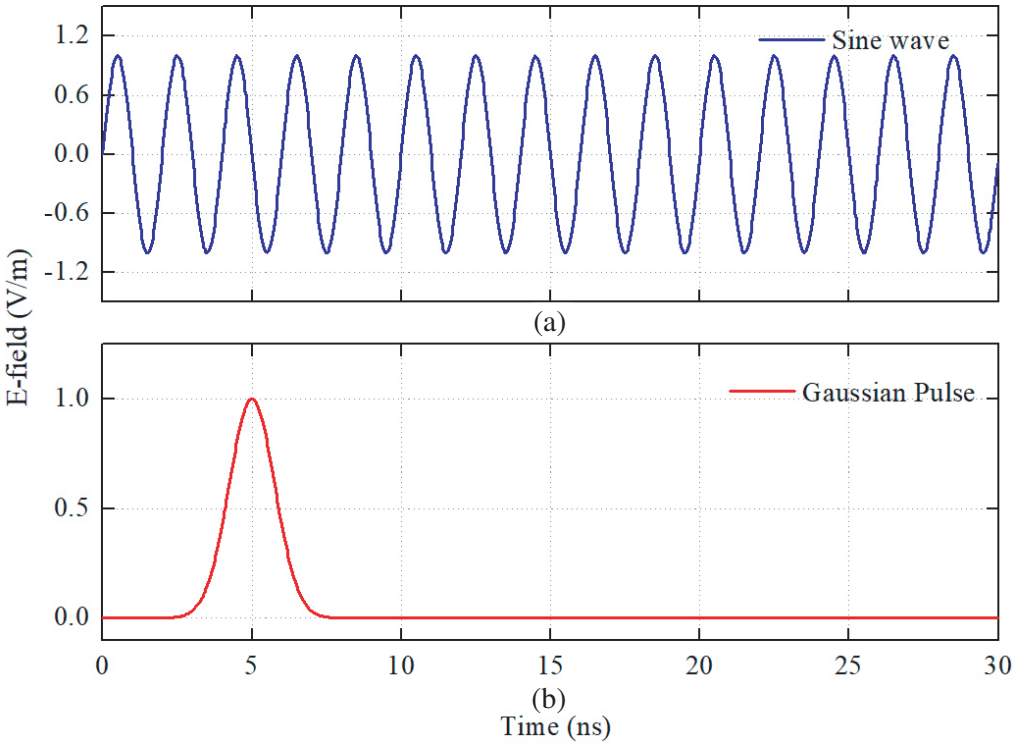

Figure 6. Influence of superposition of excitation sources on the predictability of forward scattering systems.

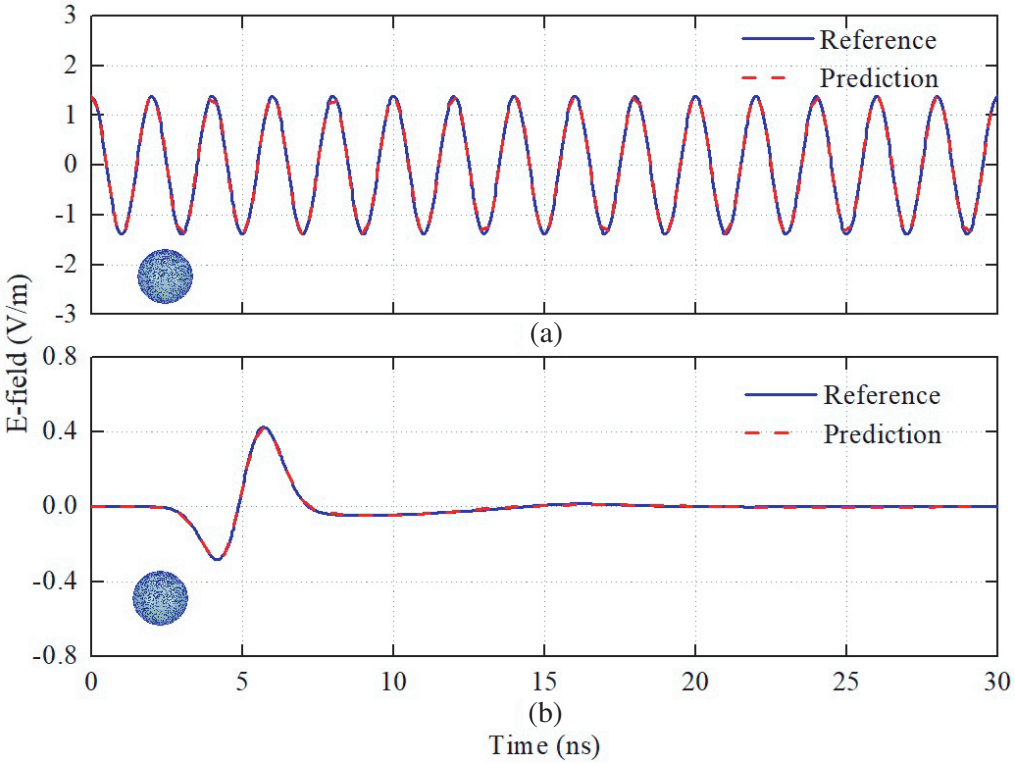

Figure 7. Influence of superposition of excitation sources on the predictability of forward scattering systems.

4. NUMERICAL EXAMPLES

4.1. Double-Obstacles Forward Scattering Prediction

To further discuss the prediction of forward scattering by this method, as shown in Fig. 8, the prediction error of forward scattering is analyzed when two scatterers are placed in parallel. We consider the two scatterers as two subsystems in a cascade, so the whole system transfer function is the product of the two subsystems. When two obstacles are far enough apart, the mutual coupling between them can be ignored. Therefore, we need to discuss the application boundaries of prediction methods.

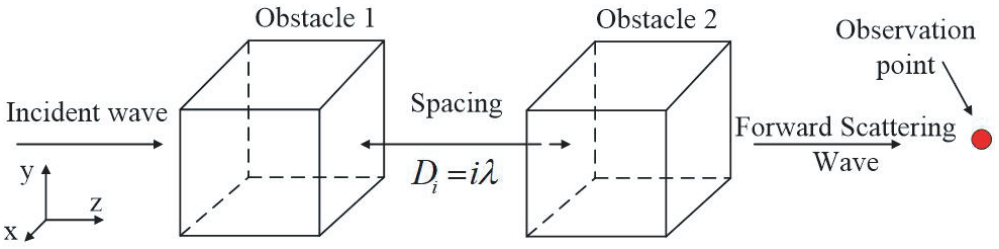

Figure 8. Schematic diagram of forward scattering of double cube obstacles.

As shown in Fig. 8, we define the distance between the two obstacles as $D_i = i\lambda$. λ represents the wavelength corresponding to the center frequency of the sinusoidal modulated Gaussian pulse excitation source. In Fig. 9, each time $i = i + 1$, a forward scattering y_i is recorded, then the current result y_i is subtracted from the previous result y_{i-1} to get error, and the max error is obtained until the calculated result is less than 0.001.

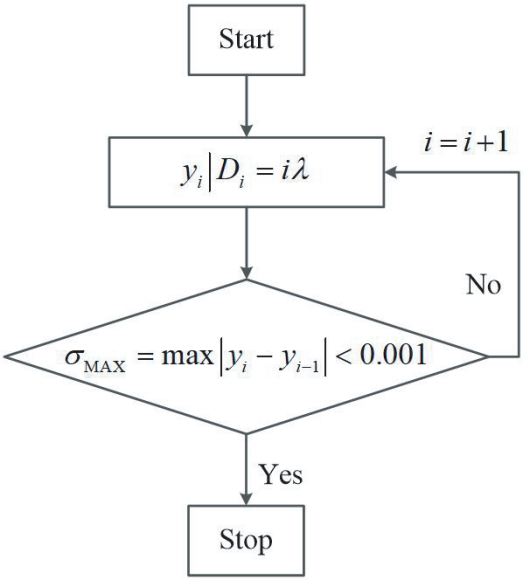

Figure 9. Flow chart of the convergence analysis of the forward scattering by the distance between obstacles.

We use CST simulation software to simulate the forward scattering results of two obstacles. The observation point is fixed, and then we change the spacing. After that, we make a deviation between the calculation results of this time and the last one. The variation of the deviation with the spacing is also discussed.

In Fig. 10, as the spacing increases, the forward scattering difference caused by the change in the distance gradually decreases. It can be considered that when the distance between two obstacles reaches

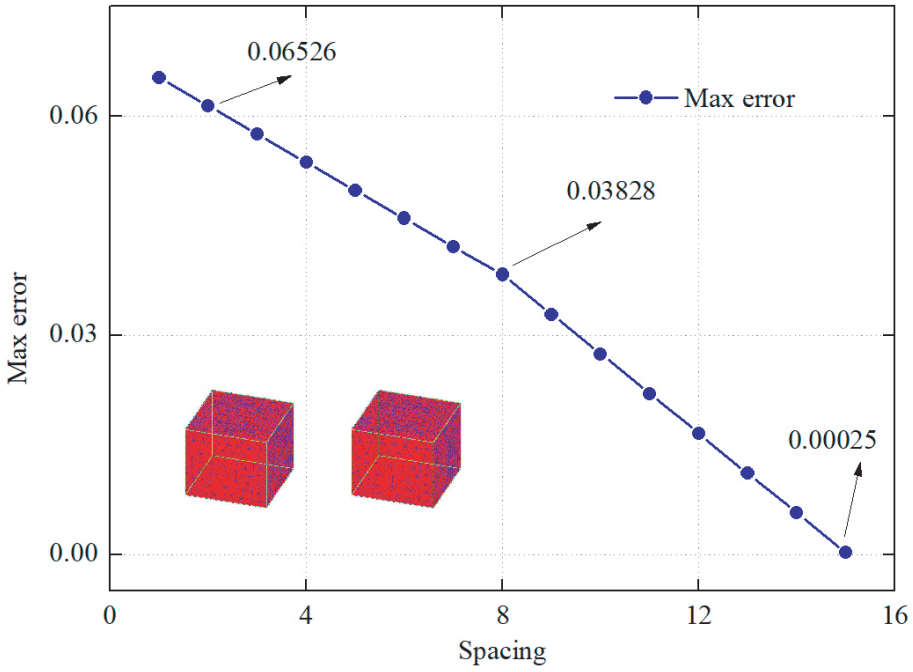

Figure 10. The influence of the change of space between two cubes on forward scattering.

more than 16λ, the error caused by the distance to the series of the subsystem transfer function can be almost ignored, and the maximum error is just under 0.00025. The result means that the coupling between the two obstacles can be neglected.

As shown in Fig. 11, we multiply the transfer functions of the two subsystems to obtain the transfer function of the double obstacles. Then the prediction results obtained by the proposed method are in good agreement with the reference obtained by CST software, and the MSE is only 0.0037, 0.0016, and 0.0008.

In addition, as shown in Table 4, for the forward scattering of the two-cube obstacle model, the CPU time and memory cost of the proposed method are only 0.15 and 0.05 times that of the DGTD method, respectively.

Table 4. Comparison of peak memory requirements and total CPU time between the proposed method and DGTD method for the forward scattering prediction of two cubes.

Methods	Total CPU time (s)	Peak memory requirement (GB)
DGTD	186	2.26
Proposed method	27	0.108

4.2. Forward Scattering Prediction of the Multiscale Obstacle

In this part, we discuss the forward scattering prediction performance of obstacles with multi-scale structures, taking the aircraft in Fig. 12 as an example.

The dimensions and electrical dimensions of the multi-scale aircraft are shown in Table 5.

According to the electric dimension of the aircraft, the aircraft model can be regarded as a multi-scale obstacle. We utilize the system identification module in MATLAB to get the system transfer function of the aircraft. Then, we use Eq. (10) to predict the forward scattering under different excitation

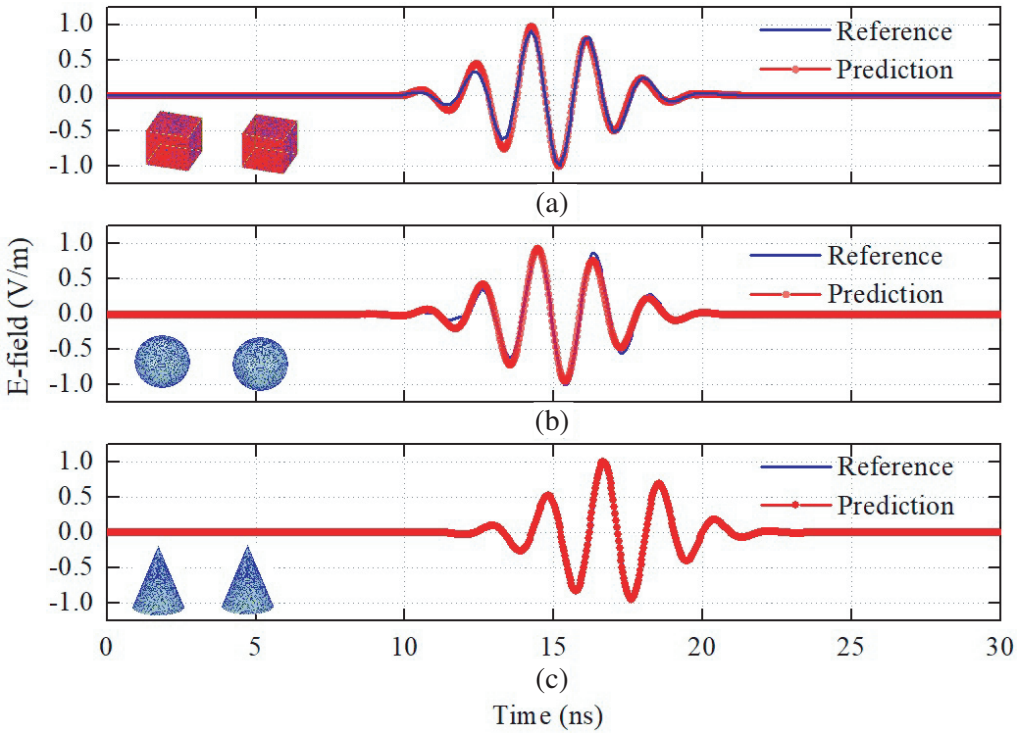

Figure 11. Forward scattering prediction of the (a) double-cubes, (b) double-spheres, (c) double-cones.

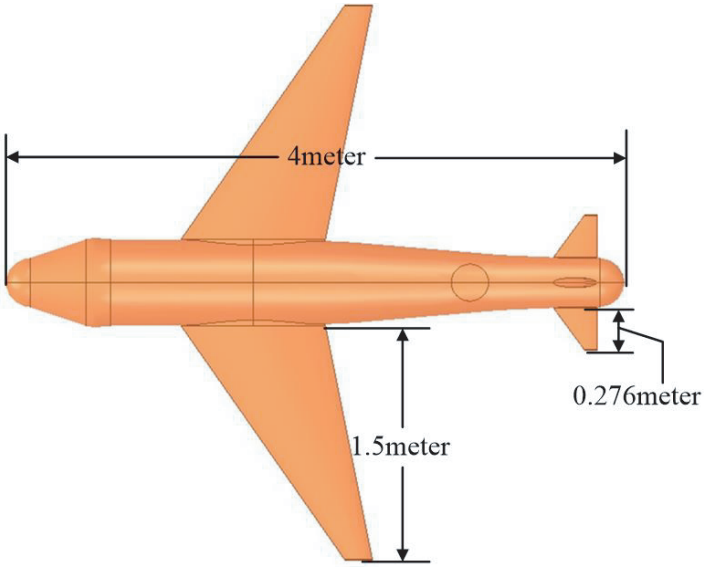

Figure 12. The aircraft model.

Table 5. Aircraft dimensions and electrical scales.

	Fuselage	Tail	Airfoil
Size	4 m	0.276 m	1.5 m
Electric scale	$10.6\lambda_{\min}$	$0.74\lambda_{\min}$	$4\lambda_{\min}$

sources.

$$STF_{\text{air}} = \frac{\begin{array}{l} 2.155 \times 10^5 z^{-1} - 1.514 \times 10^6 z^{-2} + 4.367 \times 10^6 z^{-3} \\ -6.266 \times 10^6 z^{-4} + 3.506 \times 10^6 z^{-5} - 2.418 \times 10^6 z^{-6} \\ -5.6 \times 10^6 z^{-7} + 4.134 \times 10^6 z^{-8} \\ -1.475 \times 10^6 z^{-9} + 2.141 \times 10^5 z^{-10} \end{array}}{1 - 1.983 z^{-1} - 0.9946 z^{-2}} \tag{10}$$

As shown in Fig. 13, for different excitation sources, the predicted results are in good agreement with those obtained by CST simulation software. The results in Table 6 show that the MSE of the forward scattering prediction models for multi-scale structures is all below 10^{-6}.

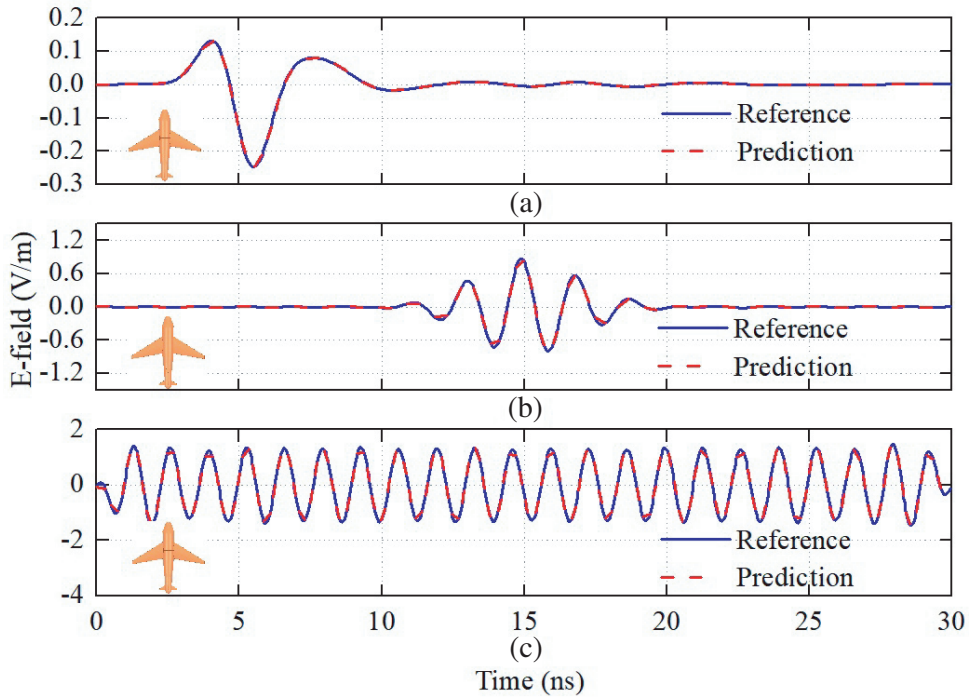

Figure 13. The prediction of forward scattering of an aircraft for (a) Gaussian pulse, (b) Sinusoidal modulated Gaussian pulse, (c) Sine wave.

Table 6. Prediction errors of aircraft forward scattering under different excitation sources.

Excitation sources	Mean Square Error (MSE)
Gaussian pulse	9.54e-6
Sinusoidal modulated Gaussian pulse	6.23e-7
Sine wave	6.45e-6

4.3. Prediction of Forward Scattering for Aircraft-cube Combination of Obstacles

In addition to the prediction of forward scattering of multi-scale obstacles, this part also discusses the prediction of forward scattering of the aircraft-cube obstacle.

As shown in Fig. 14, the proposed prediction model can effectively calculate the obstacles of the aircraft cube combination, and the prediction results are in good agreement with the reference values. Although the calculation accuracy is not as high as that of the simple structure, the MSE can reach 0.05.

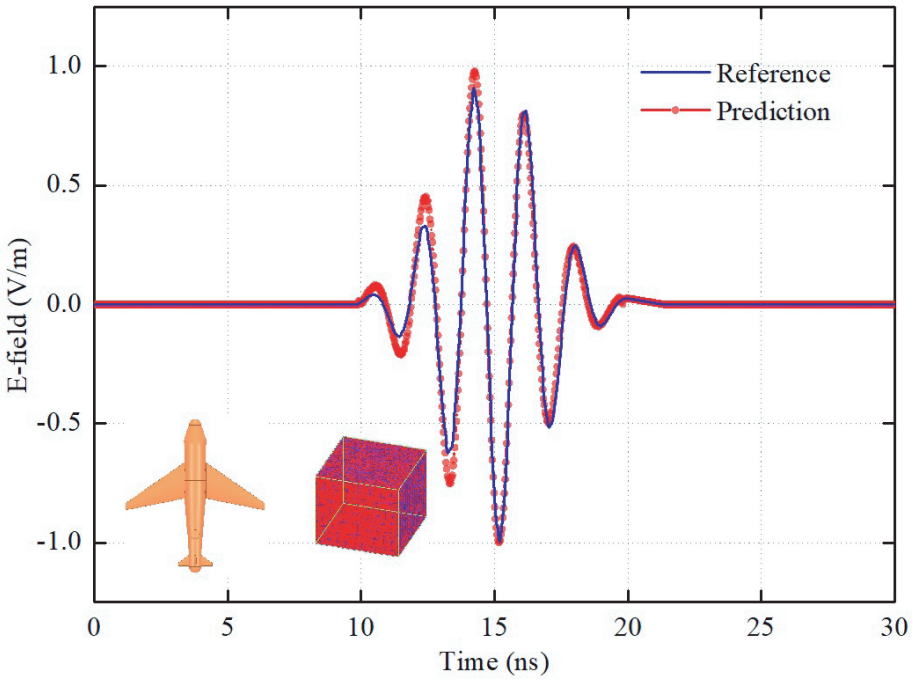

Figure 14. Prediction of forward scattering of double obstacles composed of an aircraft and a cube.

In addition, as shown in Table 7, compared with the DGTD full-wave numerical method, the CPU time of the proposed method is reduced by 71.76%, while the computational memory is reduced by 85.71%.

Table 7. Comparison of peak memory requirements and total CPU time between the proposed method and DGTD method for the aircraft-cube obstacle.

Methods	Total CPU time (s)	Peak memory requirement (GB)
DGTD	10800	10.5
Proposed method	3050	1.5

5. CONCLUSIONS

The TDPE-DGTD hybrid method is used to efficiently solve the radio wave propagation problem in the large-scale range with complex structural obstacles. Specifically, the TDPE method is used to calculate radio propagation, and the DGTD method is used to calculate forward scattering of complex structures. The discrete Laplace Z-transform is used to calculate the system transfer function of the forward scattering of obstacles, so as to realize the parallel calculation of multiple obstacles. The numerical calculation results verify the correctness of the model. Moreover, we explore the coupling between obstacles and determine the bounds of the prediction method. Simulation results show that compared with the DGTD method, the proposed model can calculate the forward scattering of multiple obstacles faster and reduce the memory cost and calculation time by 85% and 70%, respectively.

In the future, the coupling between obstacles will be fully considered on the basis of the original hybrid method, so as to broaden the application scope of TDPE-DGTD hybrid method.

ACKNOWLEDGMENT

This work was support in part by the Basic Research Business Expenses of Beijing Jiaotong University-Special Project of Frontier Science Center of Smart High Speed Railway System (number 2022JBQY003).

REFERENCES

1. Jost, T., W. Wang, U. Fiebig, and F. Pérez-Fontán, "A wideband satellite-to-indoor channel model for navigation applications," *IEEE Transactions on Antennas and Propagation*, Vol. 62, No. 10, 5307–5320, 2014.
2. Yang, L.-Q., et al., "Simulation analysis and experimental study on the echo characteristics of high-frequency hybrid sky-surface wave propagation mode," *IEEE Transactions on Antennas and Propagation*, Vol. 66, No. 9, 4821–4831, 2018.
3. Zhang, P., J. Li, H. Wang, H. Wang, and W. Hong, "Indoor small-scale spatiotemporal propagation characteristics at multiple millimeter-wave bands," *IEEE Antennas and Wireless Propagation Letters*, Vol. 17, No. 12, 2250–2254, 2018.
4. Wang, D.-D., Y.-R. Pu, X.-L. Xi, and L.-L. Zhou, "Hybrid FDTD-PE method for Loran-C ASF prediction with near-source complex topography," *IEEE Antennas and Wireless Propagation Letters*, Vol. 14, No. 2, 171–176, 2019.
5. Alzaix, B., L. Giraud, B. L. Michielsen, and J. Poirier, "A plane wave scattering dedicated integral equation," *IEEE Transactions on Antennas and Propagation*, Vol. 68, No. 2, 1088–1097, 2020.
6. El Ahdab, Z. and F. Akleman, "An efficient 3-D FDTD-PE hybrid model for radio wave propagation with near-source obstacles," *IEEE Transactions on Antennas and Propagation*, Vol. 67, No. 1, 346–355, 2019.
7. Sun, Q., Q. Ren, Q. Zhan, and Q. H. Liu, "3-D domain decomposition based hybrid finite-difference time-domain/finite-element time-domain method with nonconformal meshes," *IEEE Transactions on Microwave Theory and Techniques*, Vol. 65, No. 10, 3682–3688, 2017.
8. Bao, H. G., D. Z. Ding, and R. S. Chen, "A hybrid spectral-element finite-difference time-domain method for electromagnetic simulation," *IEEE Antennas and Wireless Propagation Letters*, Vol. 16, No. 8, 2244–2248, 2017.
9. Sun, Q., R. Zhang, Q. Zhan, and Q. H. Liu, "3-D implicit-explicit hybrid finite difference/spectral element/finite element time domain method without a buffer zone," *IEEE Transactions on Antennas and Propagation*, Vol. 67, No. 8, 5469–5476, 2019.
10. Yang, X., et al., "A flexible FEM-BEM-DDM for EM scattering by multiscale anisotropic objects," *IEEE Transactions on Antennas and Propagation*, Vol. 69, No. 12, 8562–8573, 2021.
11. Zhao, R., Y. Chen, X. -M. Gu, Z. Huang, H. Bagci, and J. Hu, "A local coupling multitrace domain decomposition method for electromagnetic scattering from multilayered dielectric objects," *IEEE Transactions on Antennas and Propagation*, Vol. 68, No. 10, 7099–7108, 2020.
12. Wang, D., et al., "Fast 3-D volume integral equation domain decomposition method for electromagnetic scattering by complex inhomogeneous objects traversing multiple layers," *IEEE Transactions on Antennas and Propagation*, Vol. 68, No. 2, 958–966, 2020.
13. Liu, S., B. Zou, L. Zhang, and S. Ren, "A multi-GPU accelerated parallel domain decomposition one-step leapfrog ADI-FDTD," *IEEE Antennas and Wireless Propagation Letters*, Vol. 19, No. 5, 816–820, 2020.
14. Moradi, M., V. Nayyeri, S. Sadrpour, M. Soleimani, and O. M. Ramah, "A 3-D weakly conditionally stable single-field finite-difference time-domain method," *IEEE Transactions on Electromagnetic Compatibility*, Vol. 62, No. 2, 498–509, 2020.
15. Huang, L., X. Wu, Z. Li, Y. Lu, M. Wang, and Y. Long, "A parallel FDTD/ADI-PE method for ultralarge-scale propagation modeling of ILS signal analysis," *IEEE Antennas and Wireless Propagation Letters*, Vol. 19, No. 12, 2245–2249, 2020.

16. Chen, J. and Q. H. Liu, "Discontinuous Galerkin time-domain methods for multiscale electromagnetic simulations: A review," *Proceedings of the IEEE*, Vol. 101, No. 2, 242–254, 2013.
17. Sullivan, D. M., "Frequency-dependent FDTD methods using Z transforms," *IEEE Transactions on Antennas and Propagation*, Vol. 40, No. 10, 1223–1230, 1992.
18. Sullivan, D. M., "Z-transform theory and the FDTD method," *IEEE Transactions on Antennas and Propagation*, Vol. 44, No. 1, 28–34, 1996.
19. Weedon, W. H. and C. M. Rappaport, "A general method for FDTD modeling of wave propagation in arbitrary frequency-dispersive media," *IEEE Transactions on Antennas and Propagation*, Vol. 45, No. 3, 401–410, 1997.
20. Sullivan, D. M., "Nonlinear FDTD formulations using Z transforms," *IEEE Transactions on Microwave Theory and Techniques*, Vol. 43, No. 3, 676–682, 1995.
21. Abraham, D. S. and D. D. Giannacopoulos, "A convolution-free mixed finite-element time-domain method for general nonlinear dispersive media," *IEEE Transactions on Antennas and Propagation*, Vol. 67, No. 1, 324–334, 2019.
22. Chakarothai, J., "Novel FDTD scheme for analysis of frequency-dependent medium using fast inverse laplace transform and Prony's Method," *IEEE Transactions on Antennas and Propagation*, Vol. 67, No. 9, 6076–6089, 2019.
23. Shibayama, K., K. Suzuki, T. Iwamoto, J. Yamauchi, and H. Nakano, "Dispersive contour-path FDTD algorithm for the Drude-Lorentz Model," *IEEE Antennas and Wireless Propagation Letters*, Vol. 19, No. 10, 1699–1703, 2020.
24. Wang, Z., L. Guo, and J. Li, "Analysis of echo characteristics of spatially inhomogeneous and time-varying plasma sheath," *IEEE Transactions on Plasma Science*, Vol. 49, No. 6, 1804–1811, 2021.
25. Han, X., H. Xu, Y. Chang, M. Lin, and X. Wei, "Investigation on the parameters distribution and electromagnetic scattering of radome inductively coupled plasma," *IEEE Transactions on Antennas and Propagation*, Vol. 69, No. 12, 8711–8721, 2021.
26. Dolean, V., H. Fah, L. Fezoui, and S. Lanteri, "Locally implicit discontinuous Galerkin method for time domain electromagnetics," *J. Comput. Phys.*, Vol. 229, No. 2, 512–526, 2010.